



## Two dansyl fluorophores bearing amino acid for monitoring $\text{Hg}^{2+}$ in aqueous solution and live cells

Chuda Raj Lohani, Joung Min Kim, Keun-Hyeung Lee \*

Bioorganic Chemistry Lab, Department of Chemistry, Inha University, 253-Yunghyun-dong, Nam-gu, Incheon 402-751, South Korea

### ARTICLE INFO

#### Article history:

Received 2 December 2010

Received in revised form 28 March 2011

Accepted 29 March 2011

Available online 9 April 2011

#### Keywords:

$\text{Hg}^{2+}$

Amino acid

Turn on

Sensor

Probe

Fluorescent

### ABSTRACT

A series of compounds (**1–4**) bearing one or two dansyl fluorophore(s) based on a Lys amino acid were synthesized in solid phase synthesis. Among them, two dansyl labeled Lys amino acid **3** detected  $\text{Hg}^{2+}$  in a 100% aqueous solution with high sensitivity ( $K_d=4.3$  nM) via a turn-on response. Compound **3** was applied for monitoring  $\text{Hg}^{2+}$  in environmental and biological fields. **3** showed a hypersensitive response to  $\text{Hg}^{2+}$  without interferences from other metal ions and satisfied the requirements for monitoring the maximum allowable level (2 ppb) of mercury ions in drinking water demanded by EPA. In addition, **3** penetrated living HeLa cells and detected intracellular  $\text{Hg}^{2+}$ . The organic spectroscopic data revealed the two sulfonamide and amide groups of **3** played a key role in stabilizing the **3**- $\text{Hg}^{2+}$  complex.

© 2011 Elsevier Ltd. All rights reserved.

### 1. Introduction

The design and development of fluorescent chemosensors for the detection of biologically and environmentally important metal ions have attracted considerable interest because they allow the prompt detection of small amounts of metal ions in the field. The detection of mercury ions in aqueous solutions has been of interest because environmental contamination of highly toxic mercury ions causes serious problems for human health and ecology.<sup>1</sup> Various types of fluorescent chemical sensors for  $\text{Hg}^{2+}$  ions have been developed.<sup>2</sup> However, there is a need for fluorescent sensors that provide both selective and sensitive detection of mercury ions in aqueous solutions via a turn-on response because most  $\text{Hg}^{2+}$  sensors suffer from at least one of the following limitations; low sensitivity in aqueous solutions, cross sensitivity toward other heavy metal ions, turn off response, and low solubility in aqueous solutions.<sup>2,3</sup> Specially, as most small chemical sensors for  $\text{Hg}^{2+}$  operated only in organic or mixed aqueous–organic solutions,<sup>4,5</sup> they show some limitation in practical use for monitoring  $\text{Hg}^{2+}$  in environmental and biological samples. Therefore, it is challenging for developing new chemosensors for  $\text{Hg}^{2+}$  with high sensitivity and selectivity, turn-on response, good water solubility, and cell permeability.

Fluorescent chemosensors consist of a fluorophore part and a receptor part, that is, responsible for recognizing analytes. A

fluorophore part converts the recognition events of the sensors into fluorescent signals. Various fluorescent chemical sensors were synthesized based on the fluorophores, such as dansyl, rhodamine, anthracene, naphthyl, and Nile blue.<sup>6</sup> The receptor part for specific target metal ions was coupled with the fluorophores for the synthesis of chemical sensors. Considering the further application of  $\text{Hg}^{2+}$  chemical sensors in environmental and biological fields, the sensors are required to have good water solubility and biological compatibility. As amino acids are water soluble and biologically compatible, it is promising that development of the new  $\text{Hg}^{2+}$  chemical sensors based on amino acids as a receptor part. The conjugation of fluorophore into the amino acids is an important step for the synthesis of new fluorescent chemical sensors based on amino acids. Among the various fluorophores, the dansyl fluorophore has been used extensively in a wide variety of fluorescent chemical sensors. The dansyl fluorophore of chemical sensors has been used to detect metal ions through chelation enhanced fluorescence (CHEF) effect and the dansyl fluorophore is sensitive to the polarity of its microenvironment via an internal charge-transfer (ICT) mechanism.<sup>6b,e,g,i,7–9</sup> Several independent research groups including us have also successfully synthesized fluorescent chemical sensors by conjugation of dansyl fluorophore with N-terminal of peptides or amino acids.<sup>10</sup>

Accordingly, in this study, we chose a Lys residue and conjugated one or two dansyl fluorophore(s) with the amino acid in solid phase synthesis to synthesize a series of compounds (**1–4**) (Fig. 1). The compounds were synthesized in solid phase synthesis using Fmoc-chemistry (Supplementary data, Scheme S1).<sup>11</sup> After cleaving the

\* Corresponding author. E-mail address: [leekh@inha.ac.kr](mailto:leekh@inha.ac.kr) (K.-H. Lee).

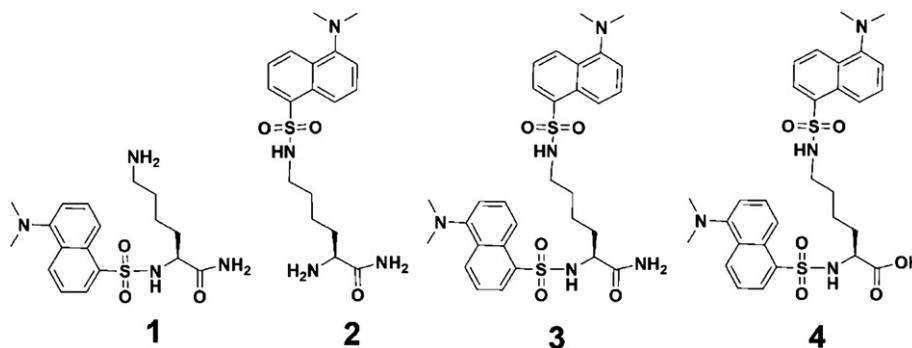


Fig. 1. Structures of 1, 2, 3, and 4.

product from the resin, the compounds were purified by semi-preparative HPLC with a  $C_{18}$  column to produce sensors with high purity. The successful synthesis and high purity (>98%) were confirmed by analytical HPLC with a  $C_{18}$  column and ESI mass spectrometer. Solid phase synthesis and HPLC purification have the advantages of rapid synthesis and high purity of the target compounds.

## 2. Result and discussion

### 2.1. Fluorescence emission response to metal ions

As all compounds showed good solubility in water, stock solutions of the compounds were prepared in 100% distilled water and all the photochemical experiments were carried out in a 100% aqueous solution without a cosolvent. Fig. 2 shows the fluorescence response of the compounds in the presence of each metal ion ( $Ca^{2+}$ ,  $Cd^{2+}$ ,  $Co^{2+}$ ,  $Pb^{2+}$ ,  $Cu^{2+}$ ,  $Ag^+$ ,  $Mg^{2+}$ ,  $Mn^{2+}$ ,  $Ni^{2+}$ ,  $Hg^{2+}$ ,  $Zn^{2+}$  as perchlorate anion and  $Na^+$ ,  $Al^{3+}$ ,  $K^+$ , as chloride anion) by excitation with 380 nm. Compounds 1 and 4 showed no fluorescent response to any metal ions, whereas 2 exhibits an excellent selectivity toward  $Cu^{2+}$  among the metal ions tested. When 1 equiv of  $Cu^{2+}$  was added, the emission intensity was considerably quenched. Interestingly, 3 exhibited outstanding selectivity toward the  $Hg^{2+}$  over other heavy and transition metal ions. 3 sensitively detected only  $Hg^{2+}$  in 100% aqueous solutions via turn-on response. When the structures of fluorescent chemical sensors containing dansyl fluorophore based

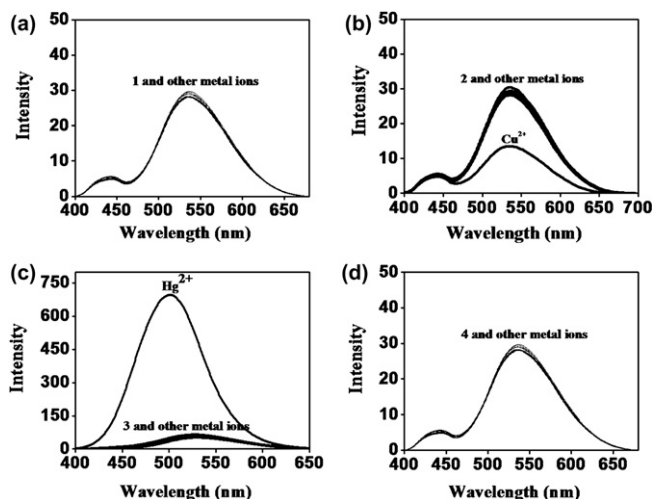


Fig. 2. Fluorescence spectra of (a) 1 (b) 2 (c) 3, and (d) 4 in 10 mM HEPES buffer solution (pH=7.4) in the presence of various metal ions (1 equiv) except  $Mg^{2+}$ ,  $Ca^{2+}$ ,  $Na^+$ , and  $K^+$ , which were used 500 equiv ( $\lambda_{ex}=380$  nm, Slit: 10/7 nm). The concentration of each compound is 10  $\mu$ M.

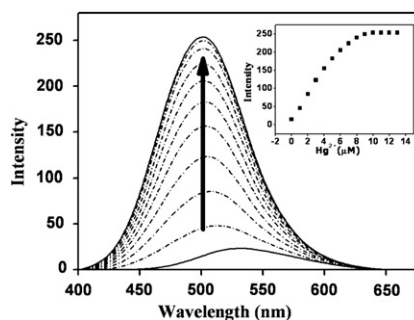


Fig. 3. Fluorescence emission spectra of 3 (8  $\mu$ M) in the presence of increasing concentrations of  $Hg^{2+}$  (0, 0.1, 0.2, 0.3, 0.4, 0.5, 0.6, 0.7, 0.8, 0.9, and 1.0 equiv).

on calix[4]arene and rhodamine were analyzed, two or four dansyl fluorophores were found to be necessary for the detection of heavy and transition metal ions, such as  $Hg^{2+}$ ,  $Pb^{2+}$ , or  $Cu^{2+}$  in aqueous solutions or aqueous–organic mixed solutions.<sup>9b,12,13</sup> Upon the addition of 1 equiv of  $Hg^{2+}$ , approximately 15-fold enhancement of the emission intensity at  $\sim 500$  nm was observed.

### 2.2. Binding stoichiometry and binding affinity

The fluorescent response of 3 to the amount of  $Hg^{2+}$  was measured in a 10 mM HEPES buffer solution at pH 7.4. As shown in Fig. 3, the emission intensity increased with increasing  $Hg^{2+}$  concentration. In the titration curve with  $Hg^{2+}$  ions,  $\sim 1$  equiv of  $Hg^{2+}$  was required for the saturation of the emission intensity of 3 (8  $\mu$ M). This suggests that although 3 has a simple structure based on a Lys residue, it has hypersensitivity to  $Hg^{2+}$  ions in a 100% aqueous solution. A Job's plot, which exhibits a maximum at a 0.5 mol fraction, indicates that the sensor forms a 1:1 complex with  $Hg^{2+}$  (Supplementary data Fig. S1). Assuming the formation of

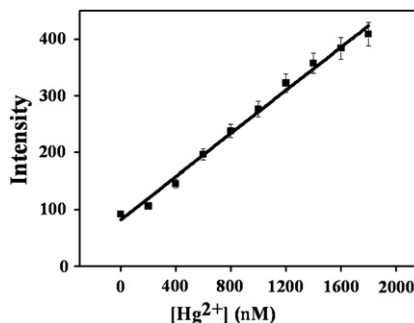
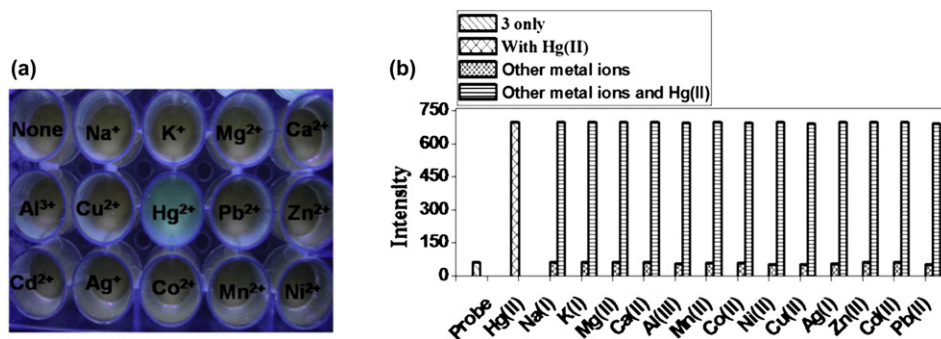


Fig. 4. Emission intensity change at 503 nm of 3 (10  $\mu$ M) with  $Hg^{2+}$  in 10 mM HEPES buffer at pH 7.4 ( $\lambda_{ex}=380$  nm, Slit: 10/3 nm).



**Fig. 5.** (a) Color emission changes of **3** (2  $\mu\text{M}$ ) upon addition of 1 equiv of various metal ions in 10 mM HEPES buffer pH 7.4 (b) Fluorescence response of **3** (10  $\mu\text{M}$ ) in the presence of  $\text{Hg}^{2+}$  (1 equiv) and additional various metal ions in 10 mM HEPES buffer (pH 7.4). All metal ions were evaluated at 1 equiv to  $\text{Hg}^{2+}$  except  $\text{Na}^+$ ,  $\text{K}^+$ ,  $\text{Ca}^{2+}$ , and  $\text{Mg}^{2+}$ , which were used at 100 equiv.

a 1:1 complex, the dissociation constant was calculated based on the titration curve with  $\text{Hg}^{2+}$  by non-linear least square fit (Supplementary data Fig. S2). The dissociation constant,  $K_d$  ( $4.28 \times 10^{-9}$  M,  $R^2=0.9621$ ), indicated that **3** has tight binding affinity to  $\text{Hg}^{2+}$  in a 100% aqueous solution. The sensitivity of **3** for  $\text{Hg}^{2+}$  was calculated on the basis of the linear relationships between the maximum emission intensity at 503 nm and the concentration of  $\text{Hg}^{2+}$ . The sensor has a detection limit of 8.7 nM (1.7 ppb), based on  $3\sigma_{\text{bi}}/m$ , where  $\sigma_{\text{bi}}$  is the standard deviation of the blank measurements, and  $m$  is the slope of the intensity versus sample concentration plot (Fig. 4). This confirms that **3** can be used to detect qualitatively low levels of  $\text{Hg}^{2+}$  in aqueous solutions. The detection limit of **3** for  $\text{Hg}^{2+}$  is lower than the maximum allowable level in drinking water (10 nM) by EPA.<sup>14</sup> The visible emission change in compound **3** was investigated in the presence and absence of  $\text{Hg}^{2+}$ . As shown in Fig. 5a, **3** (2.0  $\mu\text{M}$ ) showed a brighter color in the presence of  $\text{Hg}^{2+}$  (2.0  $\mu\text{M}$ , 1 equiv) in a 100% aqueous solution, whereas the color of **3** did not change in the presence of the other metal ions tested. According to this result, the detection limit of **3** is good enough to measure the maximum permissible concentration of mercury in blood (1.0  $\mu\text{M}$ ) and urine (3.0  $\mu\text{M}$ ).<sup>15</sup>

### 2.3. Fluorescence study in the presence of other metal ions and at different pH

The emission spectrum of **3** in the presence of  $\text{Hg}^{2+}$  and other metal ions was measured to determine the interference effect of other metal ions on the response of **3** to  $\text{Hg}^{2+}$ , Fig. 5b shows the fluorescence emission change in **3** upon the addition of each metal ion ( $\text{Ca}^{2+}$ ,  $\text{Cd}^{2+}$ ,  $\text{Co}^{2+}$ ,  $\text{Pb}^{2+}$ ,  $\text{Cu}^{2+}$ ,  $\text{Ag}^+$ ,  $\text{Mg}^{2+}$ ,  $\text{Mn}^{2+}$ ,  $\text{Ni}^{2+}$ ,  $\text{Hg}^{2+}$ ,  $\text{Zn}^{2+}$ ,  $\text{Na}^+$ ,  $\text{Al}^{3+}$ ,  $\text{K}^+$ ). The  $\text{Hg}^{2+}$  dependent fluorescence response of **3** was unaffected by the presence of Group I and II metal ions (5 mM), such as  $\text{Na}^+$ ,  $\text{K}^+$ ,  $\text{Ca}^{2+}$ , and  $\text{Mg}^{2+}$ . In particular, the fluorescence spectrum of **3**- $\text{Hg}^{2+}$  was not changed by other heavy and transition metal ions (1 equiv). The change in emission spectra after adding EDTA to the **3**- $\text{Hg}^{2+}$  complex that exhibited enhanced emission intensity was investigated to examine the reversible monitoring of  $\text{Hg}^{2+}$  (Supplementary data, Fig. S3). The addition of EDTA resulted in an instant decrease in emission intensity with 110 equiv of EDTA resulting in a return to the original metal free spectrum. EDTA is the treatment of choice to remove toxic metal ions,  $\text{Hg}^{2+}$  and  $\text{Pb}^{2+}$  in chelation therapy.<sup>16</sup> However, as EDTA also binds with essential metal ions, such as  $\text{Ca}^{2+}$ ,  $\text{Fe}^{2+}$ , and  $\text{Cu}^{2+}$ , the long-term treatment of EDTA could induce the depletion of essential minerals. Considering the more potent binding affinity than that of EDTA for  $\text{Hg}^{2+}$  and water solubility of **3**, it can be a potential candidate in chelation therapy to remove  $\text{Hg}^{2+}$ . The effect of pH influence on the fluorescence of **3** was examined in a 100% aqueous solution (Fig. 6). The maximum emission intensity of free **3** by

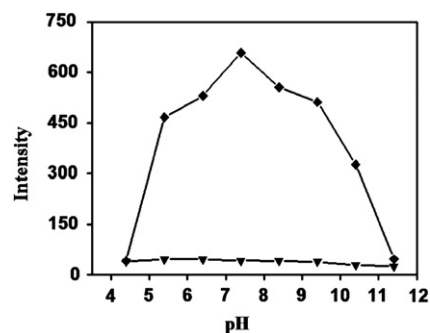


**Fig. 6.** Emission intensity of **3** in the presence (◆) and absence (▼) of  $\text{Hg}^{2+}$  (1 equiv) at different pH ( $\lambda_{\text{ex}}=380$  nm).

excitation with 380 nm was not sensitive to pH. However, the emission intensity of the **3**- $\text{Hg}^{2+}$  complex showed a dependence on pH. **3** exhibited a sensitive turn-on response to  $\text{Hg}^{2+}$  with at least 10-fold enhancements in the pH range, 5.5–9.5. The largest enhancement was observed at pH 7.5, showing that **3** is suitable for monitoring  $\text{Hg}^{2+}$  ions in physiological pH. At pH >10, the intensity of the **3**- $\text{Hg}^{2+}$  complex decreased with increasing pH. This might be due to deprotonation of the sulfonamide group  $\text{p}K_a \approx 10$  under basic conditions. Under acidic conditions, **3** and **3**- $\text{Hg}^{2+}$  complex showed very weak emission intensity. This was attributed to the protonated dimethylamino group ( $\text{p}K_a \approx 4$ ) of dansyl fluorophore, which prevents charge transfer from the dimethylamino group to the naphthyl moiety.<sup>7–9,17</sup>

### 2.4. Binding mode of **3** with $\text{Hg}^{2+}$ ion

To determine the binding mode of **3** with  $\text{Hg}^{2+}$ , the interaction between **3** and  $\text{Hg}^{2+}$  was examined using organic spectroscopy techniques, such as UV absorbance, NMR, and mass spectroscopy. The absorption spectrum of free **3** exhibited a maximum intensity at 216, 250, and 330 nm (Supplementary data, Fig. S4). Upon the addition of  $\text{Hg}^{2+}$ , a gradual red shift in the absorbance at 330 nm was observed and the absorbance at 380 nm increased. This suggests that  $\text{Hg}^{2+}$  binding to **3** resulted in an increase in the conjugation of the naphthyl moiety of the dansyl fluorophore due to an increase in the electron density of the naphthyl moiety.

NMR studies provided direct evidence of **3**- $\text{Hg}^{2+}$  interactions. As shown in Fig. 7,  $^1\text{H}$  NMR experiments were carried out in  $\text{CD}_3\text{CN}$ . The disappearance of an NH peak of the dansyl sulfonamide group at 5.7 and 6.1 ppm in the presence of  $\text{Hg}^{2+}$  (1 equiv) indicates that  $\text{Hg}^{2+}$  coordination leads to the deprotonation of NH of the sulfonamide group. N–Hg covalent bonding formation, which is in agreement

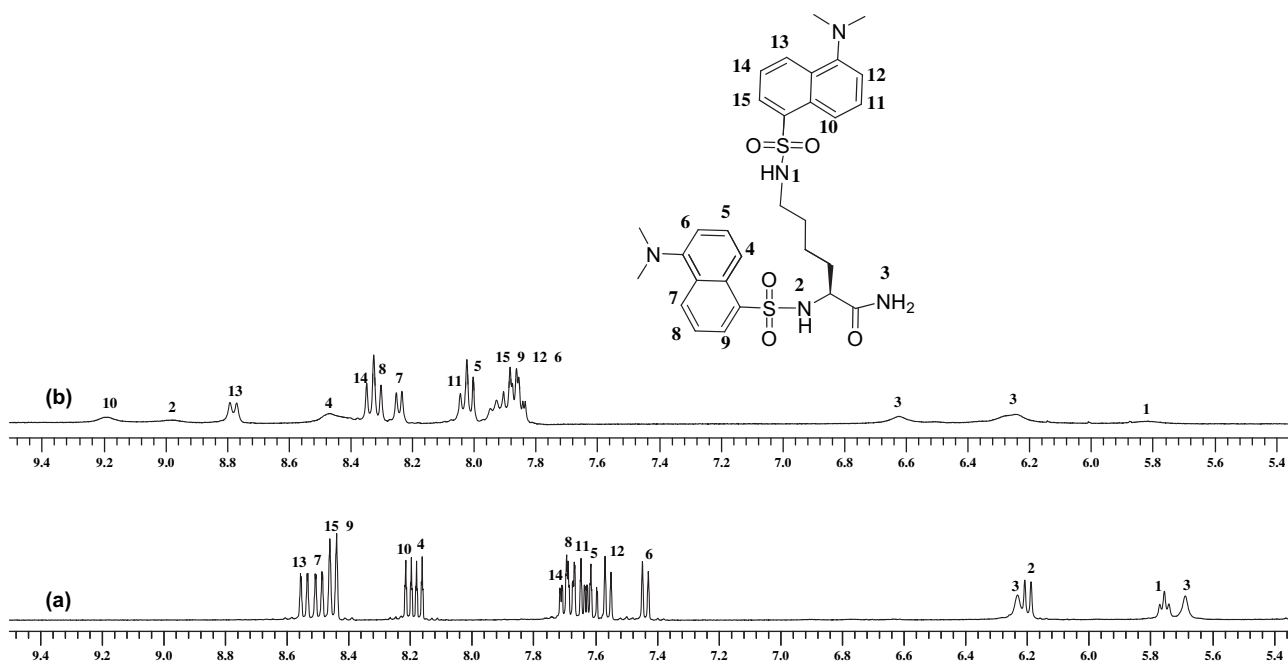
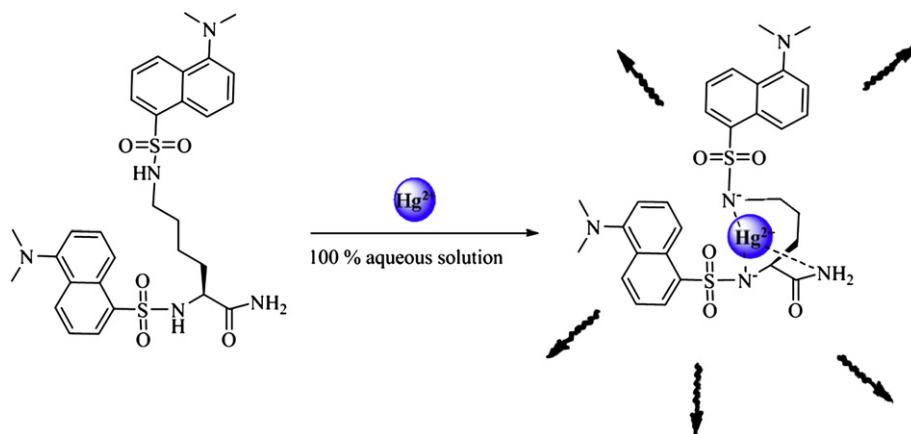


Fig. 7. Partial  $^1\text{H}$  NMR (400 MHz) of **3** (5 mM) in  $\text{CD}_3\text{CN}$  at  $25^\circ\text{C}$  (a) in the absence and (b) presence of 1 equiv of  $\text{Hg}(\text{ClO}_4)_2$ .

with the common behavior of mercury cations,<sup>18</sup> induced an increase in the electron density of the naphthyl moiety of dansyl fluorophore, resulting in a downfield shift of the aromatic protons of the dansyl fluorophore. The chelation of  $\text{Hg}^{2+}$  with the sulfonamide groups of the dansyl fluorophores increases the electron density and conjugation of the naphthyl moiety. This is, also supported by the red shift in the absorbance of **3** in the presence of  $\text{Hg}^{2+}$  (Fig. S4).

The **3**- $\text{Hg}^{2+}$  complexation was also confirmed by ESI mass spectrum (Supplementary data Fig. S5 and S6). The peak  $m/z$  612.5579 value corresponded to  $[\mathbf{3}+\text{H}^+]^+$ . When 1.0 equiv of  $\text{Hg}(\text{II})$  was added, a new peak at 810.2990 corresponding to  $[\mathbf{3}+\text{Hg}^{2+}-\text{H}^+]^+$  appeared, which indicates that **3** forms a 1:1 complex with  $\text{Hg}^{2+}$  and a deprotonation process is induced by the chelation of  $\text{Hg}^{2+}$  and **3**. The amide protons display considerable downfield shifts. This could be attributed to the shield effect, arising from binding of amide group with  $\text{Hg}^{2+}$ . To confirm the interaction between the amide group of **3** and  $\text{Hg}^{2+}$ , **4**, which has acid group instead of amide group, was synthesized and its

fluorescence response to metal ions was investigated in a 100% aqueous solution. As shown in Fig. 2, **4** showed no fluorescent response to any metal ions in aqueous solutions, indicating that the amide group of **3** plays a key role in the interaction between **3** and  $\text{Hg}^{2+}$ . As shown in IR spectra (Supplementary data Fig. S30), the disappearance of NH bands ( $3197$ ,  $2928$ , and  $2851\text{ cm}^{-1}$ ) of sulfonamide and amide groups is indicative of the participation of binding of sulfonamide and amide groups to  $\text{Hg}^{2+}$ . The small shift of  $\text{S}=\text{O}$  bands from  $1142$  to  $1112\text{ cm}^{-1}$  in the presence of  $\text{Hg}^{2+}$  suggests that  $\text{S}=\text{O}$  may not directly interact with  $\text{Hg}^{2+}$ . Based on the organic spectroscopic data, Scheme 1 presents a proposed **3**- $\text{Hg}^{2+}$  complexation structure, in which the two deprotonated sulfonamide groups cooperates with the amide group of **3** to form a stable complex between **3** and  $\text{Hg}^{2+}$ . Although two dansyl moieties containing sulfonamide groups are located at unsymmetrical positions, the two sulfonamide groups and amide group of the sensor provide sufficient interactions for the hypersensitive response to  $\text{Hg}^{2+}$  in aqueous solution.



Scheme 1. Proposed binding mode of **3** with  $\text{Hg}^{2+}$ .



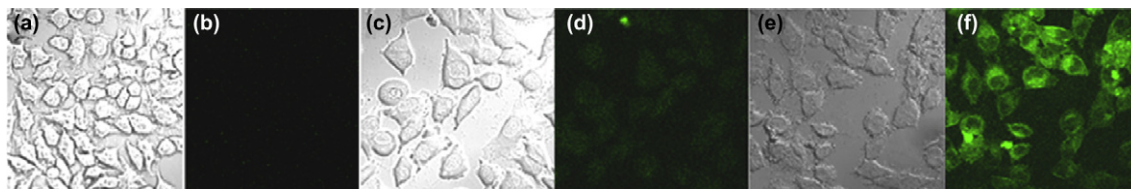


Fig. 8. Bright field (a, c, e) and confocal fluorescent (b, d, f) images of HeLa cells (a, b), HeLa cells with **3** (5  $\mu\text{M}$ ) (c, d), and HeLa cells with **3** (5  $\mu\text{M}$ ) and  $\text{Hg}^{2+}$  (20  $\mu\text{M}$ ) (e, f).

## 2.5. Sensing mercury ions in live cells

Compound **3** showed hypersensitive response to  $\text{Hg}^{2+}$  in a 100% aqueous solution because it was synthesized based on Lys amino acid, which has good water solubility. Considering the further application in the field of biology, **3** was used to monitor  $\text{Hg}^{2+}$  ions in HeLa cells to determine if the sensor can penetrate living cells and detect intracellular  $\text{Hg}^{2+}$  (Fig. 8). Compound **3** (5  $\mu\text{M}$ ) was incubated with HeLa cells for 15 min at 37  $^{\circ}\text{C}$ , and then the HeLa cells were washed with PBS. The fluorescent change in the cells was monitored by confocal microscopy. The weak fluorescent image of the cells indicates that **3** penetrated the cells. Significant increases in fluorescence intensity in HeLa cells were observed upon loading with  $\text{Hg}^{2+}$  (20.0  $\mu\text{M}$ ), demonstrating that **3** can be used to image intracellular  $\text{Hg}^{2+}$  in living cells.

## 3. Conclusion

A fluorescent sensor, **3** for  $\text{Hg}^{2+}$  was synthesized by conjugation of two dansyl fluorophores with a Lys residue. The sensor was developed based on amino acid, which is water soluble and biologically compatible. The sensor selectively and sensitively detects  $\text{Hg}^{2+}$  in aqueous buffer solutions via a turn-on response. The sensor with low detection limit of 8.7 nM (1.7 ppb) can be used to monitoring the maximum allowable level of  $\text{Hg}^{2+}$  in drinking water demanded by EPA. The largest enhancement was observed at pH 7.4, showing that **3** is suitable for monitoring  $\text{Hg}^{2+}$  ions in physiological pH. The sensor penetrated live HeLa cells and detected intracellular  $\text{Hg}^{2+}$ . The sensor penetrated live HeLa cells and detected intracellular  $\text{Hg}^{2+}$ . Therefore, it has a great potential in practical applications for monitoring low levels of  $\text{Hg}^{2+}$  contamination in environmental and biological samples. This information will be useful for the further synthesis of novel chemical sensors based on amino acids for heavy metal ions.

## 4. Experimental section

### 4.1. General

Fmoc-Lys(Fmoc)-OH and Fmoc-Lys(Boc)-OH were obtained from bead tech. Boc-Lys(Fmoc)-OH, *N,N'*-diisopropylcarbodiimide, 1-hydroxybenzotriazole, and Rink Amide MBHA resin were from advanced chem tech. Other reagents for solid phase synthesis including trifluoroacetic acid (TFA), triisopropylsilane (TIS), dansyl chloride, triethylamine, diethyl ether, *N,N'*-dimethylformamide (DMF), and piperidine were purchased from Aldrich.

### 4.2. Solid phase synthesis of compounds

Compounds were synthesized by solid phase synthesis with Fmoc chemistry.<sup>11</sup> Fmoc protected L-Lys residue was assembled on Rink Amide MBHA resin for compounds **1**, **2**, **3**, and on 2-Cl trityl resin for compound **4** (Supplementary data, Scheme S1). After deprotection of Fmoc group, the coupling of dansyl chloride was performed by the following procedure. To the resin bound amino acid (65 mg, 0.05 mmol), dansyl chloride (40 mg, 0.15 mmol,

3 equiv) in DMF (3 mL), and triethylamine (20  $\mu\text{l}$ , 0.15 mmol, 3 equiv) were added. Cleavage of the peptide from the resin was achieved by treatment with a mixture of 3 mL TFA:TIS:H<sub>2</sub>O (95:2.5:2.5 v/v/v) at room temperature for 3 h. After filtration and washing of the resin by TFA, a gentle stream of nitrogen was used to remove the excess TFA. The crude was triturated with diethyl ether chilled at  $-20$   $^{\circ}\text{C}$  and then centrifuged at 3000 rpm for 10 min at  $-10$   $^{\circ}\text{C}$ . The crude product was purified by prep-HPLC with a Vydac C<sub>18</sub> column using a water (0.1% TFA)–acetonitrile (0.1% TFA) gradient to give >97% yield. The successful synthesis was confirmed by ESI mass spectrometry (Platform II, micromass, Manchester, UK) and its homogeneity (>98%) was confirmed by reverse phase analytical HPLC with a C<sub>18</sub> column:

**4.2.1. Compound 1.** <sup>1</sup>H NMR (DMSO-*d*<sub>6</sub>)  $\delta$  8.44 (d, 1H, *J*=8.4 Hz), 8.28 (d, 1H, *J*=8.4 Hz), 8.07 (d, 1H, *J*=7.2 Hz), 7.98 (b, 2H), 7.88–7.85 (t, 1H, *J*=6 Hz), 7.77 (s, 1H), 7.63–7.55 (m, 2), 7.51 (s, 1H), 7.25 (d, 1H, *J*=7.6 Hz), 3.61 (d, 1H, *J*=5.6 Hz), 2.82 (s, 6H), 2.77–2.70 (br s, 2H), 1.60–1.56 (m, 2H), 1.37–1.34 (m, 2H), 1.26–1.22 (m, 2H); <sup>13</sup>C NMR (DMSO-*d*<sub>6</sub>)  $\delta$  170.31, 151.24, 135.97, 129.31, 129.07, 129.01, 128.14, 127.82, 124.81, 123.59, 119.14, 115.16, 45.07, 42.20, 30.39, 28.81, 21.30; mp 211–213  $^{\circ}\text{C}$ ; ESI-MS: calcd 379.17, obsd 379.09 [M+H]<sup>+</sup>. Anal. Calcd for C<sub>18</sub>H<sub>26</sub>N<sub>4</sub>O<sub>3</sub>S: C, 57.12; H, 6.92; N, 14.80; S, 8.47. Found: C, 57.23; H, 6.97; N, 14.87; S, 8.41.

**4.2.2. Compound 2.** <sup>1</sup>H NMR (DMSO-*d*<sub>6</sub>)  $\delta$  8.60 (1H, *J*=8.4 Hz), 8.48 (1H, *J*=8 Hz), 8.30–8.26 (m, 2H), 7.83 (br s, 2H), 7.77–7.72 (m, 2H), 7.39 (d, 1H, *J*=7.8 Hz), 7.35 (s, 1H), 7.09 (s, 1H), 3.74 (m, 1H), 3.0 (s, 6H), 2.66–2.59 (m, 2H), 1.63–1.54 (m, 2H), 1.44–1.39 (m, 2H), 1.26–1.24 (m, 1H), 1.12–1.11 (m, 1H); <sup>13</sup>C NMR (DMSO-*d*<sub>6</sub>)  $\delta$  170.36, 151.29, 136.02, 129.36, 129.13, 129.07, 128.20, 127.87, 123.65, 119.19, 115.22, 45.12, 42.25, 30.44, 28.86, 21.35; mp 213–215  $^{\circ}\text{C}$ ; ESI-MS: calcd 379.17, obsd 379.09 [M+H]<sup>+</sup>. Anal. Calcd for C<sub>18</sub>H<sub>26</sub>N<sub>4</sub>O<sub>3</sub>S: C, 57.12; H, 6.92; N, 14.80; S, 8.47. Found: C, 57.26; H, 6.87; N, 14.76; S, 8.38.

**4.2.3. Compound 3.** <sup>1</sup>H NMR (DMSO-*d*<sub>6</sub>)  $\delta$  8.46 (d, 1H, *J*=8.4 Hz), 8.35 (d, 1H, *J*=8.8 Hz), 8.28–8.23 (m, 2H), 8.08–8.00 (m, 3H), 7.71 (s, 1H), 7.63 (s, 1H), 7.57–7.48 (m, 3H), 7.27 (d, 1H, *J*=7.6 Hz), 7.12 (d, 2H, *J*=6.0 Hz), 6.88 (s, 1H), 3.5 (m, 1H), 2.9 (s, 6H), 2.7 (s, 6H), 2.4 (m, 2H), 1.2 (m, 2H), 1.0 (m, 1H), 0.9 (br s, 2H), 0.6 (m, 1H); <sup>13</sup>C NMR (DMSO-*d*<sub>6</sub>)  $\delta$  173.00, 158.52, 158.18, 150.20, 150.08, 136.19, 136.09, 129.12, 128.98, 128.73, 128.61, 128.44, 128.24, 127.71, 127.54, 123.81, 123.59, 120.09, 119.80, 115.52, 1155.32, 55.02, 45.18, 45.08, 41.81, 31.012, 28.10, 21.76; mp 183–184  $^{\circ}\text{C}$ ; ESI-MS: calcd 612.22, obsd 612.55 [M+H]<sup>+</sup>. Anal. Calcd for C<sub>30</sub>H<sub>37</sub>N<sub>5</sub>O<sub>5</sub>S<sub>2</sub>: C, 58.90; H, 6.10; N, 11.45; S, 10.48. Found: C, 58.81; H, 6.16; N, 11.39; S, 10.54.

**4.2.4. Compound 4.** <sup>1</sup>H NMR (DMSO-*d*<sub>6</sub>) 8.46(d, 1H, *J*=8.8 Hz), 8.37–8.34 (m, 2H), 8.32–8.27 (m, 2H), 8.07(d, 1H, *J*=7.2 Hz), 8.03 (d, 1H, *J*=3.6 Hz), 7.3 (t, 1H, *J*=2.8 Hz), 7.66–7.49 (m, 4H), 7.32 (d, 1H, *J*=7.6 Hz), 7.18 (d, 1H, *J*=7.6 Hz), 7.18 (d, 1H, *J*=7.6 Hz), 3.41(q, 1H, *J*=7.6 Hz), 2.80 (s, 6H), 2.75 (s, 6H), 2.32–2.24 (m, 2H), 1.32–1.26 (m, 2H), 1.21 (s, 1H), 0.92–0.85 (m, 3H); <sup>13</sup>C NMR (DMSO-*d*<sub>6</sub>)  $\delta$  173.06, 158.06, 158.23, 150.25, 150.13, 136.25, 136.15, 129.18, 129.04, 128.79, 128.67, 128.49, 128.29, 127.76, 127.59, 123.86, 123.64, 120.15, 119.86, 115.57, 115.38, 55.08, 45.24, 45.14, 41.86, 31.06, 28.16, 21.81; mp

186–187 °C; ESI-MS: calcd 612.22, obsd 612.55 [M+H]<sup>+</sup>. Anal. Calcd for C<sub>30</sub>H<sub>36</sub>N<sub>4</sub>O<sub>6</sub>S<sub>2</sub>: C, 58.80; H, 5.92; N, 9.14; S, 10.47. Found: C, 58.88; H, 5.83; N, 9.22; S, 10.38.

### 4.3. General fluorescence measurements

The stock solution of compound **3** and **4** was prepared by dissolving ~1 mg of **3** or **4** in 4 mL of distilled water with 5 μL (0.125% v/v) of TFA. The concentration of compound was confirmed by UV absorbance and was diluted into 10 mM HEPES buffer solution for the fluorescence measurement. Fluorescence emission spectrum of a probe in a 10 mm path length quartz cuvette was measured in 10 mM HEPES buffer solution (pH 7.4) using a Perkin–Elmer luminescence spectrophotometer (model LS 55). Emission spectra of the probe (10 μM) in the presence of various metal ions (Hg<sup>2+</sup>, Ca<sup>2+</sup>, Cd<sup>2+</sup>, Co<sup>2+</sup>, Pb<sup>2+</sup>, Ag<sup>+</sup>, Mg<sup>2+</sup>, Cu<sup>2+</sup>, Mn<sup>2+</sup>, Ni<sup>2+</sup>, and Zn<sup>2+</sup> as perchlorate anion; and Na<sup>+</sup>, Al<sup>3+</sup>, and K<sup>+</sup>, as chloride anion) were measured by excitation with 380 nm. The slit size for excitation and emission was 10 and 3 nm, respectively. The concentration of the probe was confirmed by UV absorbance at 330 nm for dansyl group.

### 4.4. Determination of dissociation constant and detection limit

The dissociation constant was calculated based on the titration curve of the probe with metal ion. The fluorescence signal, F, is related to the equilibrium concentration of the complex (HL) between Host (H) and metal ion (L) by the following expression:

$$F = F_0 + \Delta F \times [\text{HL}]$$

$$[\text{HL}] = 0.5 \times \left[ K_D + L_T + H_T - \left\{ (-K_D - L_T - H_T)^2 - 4L_T H_T \right\}^{1/2} \right]$$

Where F<sub>0</sub> is the fluorescence of the probe only and ΔF is the change in fluorescence due to the formation of HL. Association constants were determined by a non-linear least squares fit of the data with the equation.<sup>19</sup>

The detection limit was calculated based on the fluorescence titration. To determine the S/N ratio, the emission intensity of **3** without any metal ions was measured by ten times and the standard deviation of blank measurements was determined. Three independent duplication measurements of emission intensity were performed in the presence of metal ions and each average value of the intensities was plotted as a concentration of metal ions for determining the slope. The detection limit is then calculated with the following equation.

$$\text{Detection limit} = 3\sigma_{\text{bi}}/m$$

Where σ<sub>bi</sub> is the standard deviation of blank measurements, m is the slope between intensity versus sample concentration.

### 4.5. Detection of Hg<sup>2+</sup> in live cells

HeLa cells were cultured according to the reported protocol.<sup>20</sup> Cell imaging experiments were performed with a LSM 510 META confocal laser-scanning fluorescent microscope (ZEISS, German) with 20× objective lens. Excitation at 405 nm was carried out with an argon ion laser. HeLa cells were attached to the plate 24 h before study. After cells were treated with 5 μM of **3** containing 2% DMSO for 10 min at 37 °C and then washed twice with PBS. The weak fluorescent intensity of the cells was confirmed and then the cells were further incubated in 20 μM Hg(ClO<sub>4</sub>)<sub>2</sub> in PBS for 10 min. Cells

were washed three times with PBS and confocal fluorescent microscopy was recorded for them.

### Acknowledgements

This work was supported by the grant (2009-0076572) from the Basic Research Program of National Research Foundation of Korea.

### Supplementary data

Experimental procedure and characterization data of compounds are presented in Supplementary data. Supplementary data related to this article can be found online at doi:10.1016/j.tet.2011.03.106.

### References and notes

- (a) Hutchinson, T. C.; Meema, K. M. *Lead, Mercury, Cadmium and Arsenic in the Environment*; Wiley, J: New York, NY, 1987; (b) *Mercury, Cadmium, and Lead: Handbook for Sustainable Heavy Metals Policy and Regulation*; Scollos, G. H., Vonkeman, M. J., Thorton, L., Makuch, Z., Eds. Environment & Policy; Kluwer Academic: Norwell, MA, 2001; Vol. 31; (c) Coester, C. J. *Anal. Chem.* **2005**, *77*, 3737; (d) Richardson, S. D.; Temes, T. A. *Anal. Chem.* **2005**, *77*, 3807; (e) *Mercury Update: Impact on Fish Advisories. EPA Fact Sheet EPA-823-F-01-011*; EPA, Office of Water: Washington, DC, 2001.
- (a) Nolan, E. M.; Lippard, S. J. *Chem. Rev.* **2008**, *108*, 3443; (b) Coskun, A.; Yilmaz, M. D.; Akkaya, E. U. *Org. Lett.* **2007**, *9*, 607; (c) Liu, B.; Tian, H. *Chem. Commun.* **2005**, 3156; (d) Zhu, X. J.; Fu, S. T.; Wong, W. K.; Guo, H. P.; Wong, W. Y. *Angew. Chem., Int. Ed.* **2006**, *45*, 3150; (e) Zheng, H.; Qian, Z. H.; Xu, L.; Yuan, F. F.; Lan, L. D.; Xu, J. G. *Org. Lett.* **2006**, *8*, 859; (f) Chen, P.; He, C. J. *Am. Chem. Soc.* **2004**, *126*, 728; (g) Ono, A.; Togashi, H. *Angew. Chem., Int. Ed.* **2004**, *43*, 4300; (h) Wu, J. S.; Hwang, I. C.; Kim, K. S.; Kim, J. S. *Org. Lett.* **2007**, *9*, 907; (i) Chen, X.; Baek, K.; Kim, Y.; Kim, S.; Shin, I.; Yoon, J. *Tetrahedron* **2010**, *66*, 4016; (j) Suresh, M.; Mandal, A. K.; Saha, S.; Suresh, E.; Mandoli, A.; Liddo, R. D.; Parnigotto, P. P.; Das, A. *Org. Lett.* **2010**, *12*, 5406; (k) Mahato, P.; Ghosh, A.; Saha, S.; Mishra, S.; Mishra, S. K.; Das, A. *Inorg. Chem.* **2010**, *49*, 11285.
- (a) Wang, J.; Qian, X.; Cui, J. *J. Org. Chem.* **2006**, *71*, 4308; (b) Nolan, E. M.; Lippard, S. J. *J. Mater. Chem.* **2005**, *15*, 2778; (c) Nolan, E. M.; Lippard, S. J. *J. Am. Chem. Soc.* **2007**, *129*, 5910.
- (a) Zhou, Y.; Zhu, C.-Y.; Gao, X.-S.; You, X.-Y.; Yao, C. *Org. Lett.* **2010**, *12*, 2566; (b) Hennrich, G.; Sonnenschein, H.; Resch-Genger, U. *J. Am. Chem. Soc.* **1999**, *121*, 5073; (c) Zhang, G.; Zhang, D.; Yin, S.; Yang, X.; Shuai, Z.; Zhu, D. *Chem. Commun.* **2005**, 2161; (d) Resch, U.; Rurack, K.; Bricks, J. L.; Slominski, J. L. *J. Fluoresc.* **1997**, *7*, 231; (e) Rurack, K.; Resch-Genger, U.; Bricks, J. L.; Spieles, M. *Chem. Commun.* **2000**, 2103.
- (a) Dhir, A.; Bhalla, V.; Kumar, M. *Org. Lett.* **2008**, *10*, 4891; (b) Kim, S. H.; Youn, N. J.; Park, J. Y.; Choi, M. G.; Chang, S.-K. *Bull. Korean Chem. Soc.* **2006**, *27*, 1553; (c) Sakamoto, H.; Ishikawa, J.; Nakao, S.; Wada, H. *Chem. Commun.* **2001**, 2395; (d) Guo, X.; Qian, X.; Jia, L. *J. Am. Chem. Soc.* **2004**, *126*, 2272; (e) Kim, S. H.; Kim, J. S.; Park, J. S.; Chang, S.-K. *Org. Lett.* **2006**, *8*, 371.
- (a) Guo, W.; Yuan, J.; Wang, E. *Chem. Commun.* **2009**, 3395; (b) Wang, Z.; Lee, J. H.; Lu, Y. *Chem. Commun.* **2008**, 6005; (c) Yang, R.; Jin, J.; Long, L.; Wang, L.; Wang, H.; Tan, W. *Chem. Commun.* **2009**, 322; (d) Tian, M.; Ihmels, H. *Chem. Commun.* **2009**, 3175; (e) Li, H.; Li, Y.; Dang, Y.; Ma, L.; Wu, Y.; Hou, G.; Wu, L. *Chem. Commun.* **2009**, 4453; (f) Jana, A.; Kim, J. S.; Jung, H. S.; Bharadwaj, P. K. *Chem. Commun.* **2009**, 4417; (g) Joshi, B. P.; Lohani, C. R.; Lee, K. H. *Org. Biomol. Chem.* **2010**, *8*, 3220; (h) Yoon, S.; Miller, E. W.; He, Q.; Do, P. H.; Chang, C. J. *Angew. Chem., Int. Ed.* **2007**, *46*, 6658; (i) Ma, L.; Li, Y.; Li, L.; Sun, J.; Tian, C.; Wu, Y. *Chem. Commun.* **2008**, 6345.
- (a) Leray, I.; Lefevre, J. P.; Delouis, J. F.; Delaire, J.; Valeur, B. *Chem.—Eur. J.* **2001**, *7*, 4590; (b) Balzani, V.; Ceroni, P.; Gestermann, S.; Kauffmann, C.; Gorka, M.; Vogtle, F. *Chem. Commun.* **2000**, 853; (c) Vogtle, F.; Gestermann, S.; Kauffmann, C.; Ceroni, P.; Vicinelli, V.; Balzani, V. *J. Am. Chem. Soc.* **2000**, *122*, 10398; (d) Deo, S.; Godwin, H. A. *J. Am. Chem. Soc.* **2000**, *122*, 174.
- (a) Aoki, S.; Kawatani, H.; Goto, T.; Kimura, E.; Shiro, M. *J. Am. Chem. Soc.* **2001**, *123*, 1123; (b) Kimura, E.; Koike, T. *Chem. Soc. Rev.* **1998**, *27*, 179; (c) Haugland, R. P. *Molecular Probes*, 6th ed.; Wiley, J. Eugene; 1996; (d) Kavallieratos, K.; Rosenberg, J. M.; Chen, W.; Ren, T. *J. Am. Chem. Soc.* **2005**, *127*, 6514.
- (a) Zheng, Y.; Gattas-Asfura, K. M.; Konak, V.; Leblanc, R. M. *Chem. Commun.* **2002**, 2350; (b) Métivier, R.; Leray, I.; Valeur, B. *Photochem. Photobiol. Sci.* **2004**, *3*, 374; (c) Métivier, R.; Leray, I.; Valeur, B. *Chem.—Eur. J.* **2004**, *10*, 4480.
- (a) Joshi, B. P.; Park, J. W.; Lee, K. H. *Talanta* **2009**, *78*, 903; (b) White, B. R.; Liljestrand, H. M.; Holcombe, J. A. *Analyst* **2008**, *133*, 65; (d) Joshi, B. P.; Cho, W. M.; Kim, J. S.; Yoon, J. Y.; Lee, K. H. *Bioorg. Med. Chem. Lett.* **2007**, *17*, 6425; (e) Joshi, B. P.; Lee, K. H. *Bioorg. Med. Chem.* **2008**, *16*, 8501; (f) Walkup, G. K.; Imperiali, B. *J. Am. Chem. Soc.* **1996**, *118*, 3053; (g) Cheng, R. P.; Fischer, S. L.; Imperiali, B. *J. Am. Chem. Soc.* **1996**, *118*, 11349.
- Fields, G. B.; Nobel, G. B. *Int. J. Pept. Protein Res.* **1990**, *35*, 161.
- Koike, T.; Watanabe, T.; Aoki, S.; Kimura, E.; Shiro, M. *J. Am. Chem. Soc.* **1996**, *118*, 12696.
- Lee, M. H.; Wu, J.; Lee, J. W.; Jung, J. H.; Kim, J. S. *Org. Lett.* **2007**, *9*, 2501.

14. (a) *Guidelines for Drinking-Water Quality*, 3rd ed.; World Health Organization: Geneva, 2004; 188; (b) US Environmental Protection Agency, EPA Office of Water, Washington (<http://www.epa.gov/ogwdw000/contaminants/index.html#mcls>).
15. (a) Liu, L. X.; Weller, P. F. In *Harrison's Principles of Internal Medicine*; Fauci, A. S., et al., Eds.; McGraw-Hill: New York, NY, 1997; (b) Food and Drug Administration. Office of Inquiry and Consumer Information. 5600 Fisher Lane, Room 12-A-40, Rockville, MD 20857 (301) 827–4420. <http://www.fda.gov/fdahomepage.html>.
16. (a) Burns, C. B.; Currie, B. *Aust. N. Z. J. Med.* **1995**, 25, 197; (b) Chappell, L. T.; Wilson, J. *Circulation* **1999**, 99, 164.
17. O'Connor, N. A.; Sakata, S. T.; Zhu, H.; Shea, K. J. *Org. Lett.* **2006**, 8, 1581.
18. Hancock, R. D.; Martell, A. E. *Chem. Rev.* **1989**, 89, 1875.
19. Reddi, A. R.; Guzman, T. R.; Breece, R. M.; Tierney, D. L.; Gibney, B. R. *J. Am. Chem. Soc.* **2007**, 129, 12815.
20. Taki, M.; Desaki, M.; Ojida, A.; Iyoshi, S.; Hirayama, T.; Hamachi, I.; Yamamoto, Y. *J. Am. Chem. Soc.* **2008**, 130, 12564.